Science Press

ARTICLE

# Fabrication of Anhydrous AlF$_3$ by Fluorination of Al$_2$O$_3$ Using NH$_4$HF$_2$

**Li Chengshuo,   Meng Junsheng,   Chen Mingxuan,   Shi Xiaoping,   Li Xiao,   Ma Qiang**

*College of Naval Architecture and Port Engineering, Shandong Jiaotong University, Weihai 264200, China*

**Abstract:** The thermal behavior of Al$_2$O$_3$/NH$_4$HF$_2$ mixtures with different mass ratios of NH$_4$HF$_2$: Al$_2$O$_3$ were analyzed by simultaneous thermogravimetry and differential thermal analysis (TG-DTA) and the critical temperature of DTA curve were determined. The morphologies and phases of the products obtained by direct thermal treatment before and after each critical temperature were further analyzed. The results show that the mass ratio has no influence on the critical reaction temperature and processes. The fluorination starts at room temperature with the formation of (NH$_4$)$_3$AlF$_6$, which dominates at 162.3~162.8 °C and is completed around 180 °C. After further heat-treatment, (NH$_4$)$_3$AlF$_6$ decomposes sequentially through a two-step decomposition reaction with the formation of NH$_4$AlF$_4$ at 249.8~250.1 °C and finally decomposes to $\beta$-AlF$_3$ at 356.8~357.7 °C. The transformation of $\beta$-AlF$_3$ to $\alpha$-AlF$_3$ occurs at 400~650 °C.

**Key words:** ammonium bifluoride; fluorination; thermal decomposition; aluminium fluoride

Anhydrous AlF$_3$ can be used as cathode materials for lithium battery[1,2], fluoride fiber materials[3] or raw materials related to aluminum electrolyte[4]. However, AlF$_3$ prepared through hydrometallurgical process always contains crystal water. If heating aluminum fluoride containing crystal water, alumina will be formed because of the hydrolysis reaction of aluminum fluoride[5,6]. Therefore, it is important to develop a process for preparing pure AlF$_3$ without water. Sublimation under vacuum is commonly used[7], but the experimental equipment is strictly required. Anhydrous fluorides can be prepared by a non-aqueous dry route through the fluorination of metal or oxides using fluorine gas (F$_2$)[8], hydrogen fluoride gas (HF)[9,10], aqueous hydrofluoric acid (HF)[11,12], ammonium fluoride (NH$_4$F) [13] and ammonium bifluoride (NH$_4$HF$_2$) [14,15]. Among them, fluorine, hydrogen fluoride and aqueous hydrofluoric acid are corrosive and poisonous gases, and thus are difficult to handle. NH$_4$F is highly hygroscopic and there is a possibility for oxygen contamination[16,17]. Thus, a large quantity of NH$_4$F should be added in order to produce a pure fluoride[13]. Therefore, NH$_4$HF$_2$ is considered as an appropriate fluorination agent for obtaining high pure fluoride because HF generated by the decomposition of NH$_4$HF$_2$ will inhibit the hydrolysis of aluminum fluoride. The melting and decomposition point of NH$_4$HF$_2$ is 126.8 and 238.8 ° C, respectively. NH$_4$HF$_2$ is a solid without any environmental danger at room temperature; whereas it becomes a powerful fluorinating reagent when heated. It is reported that NH$_4$HF$_2$ can react with different Al$_2$O$_3$-containing minerals such as beryl[15], nepheline[18], non-bauxite[19], kyanite[20,21] and $\alpha$ - spodumene[22] to form (NH$_4$)$_3$AlF$_6$ or NH$_4$AlF$_4$ according to following reactions:

$$Al_2O_3+6NH_4HF_2=2(NH_4)_3AlF_6+3H_2O \uparrow \qquad (1)$$
$$Al_2O_3+4NH_4HF_2=2NH_4AlF_4+2NH_3 \uparrow +3H_2O \uparrow \qquad (2)$$
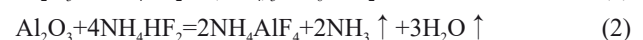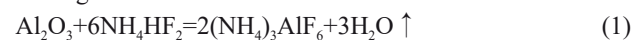
After further heat-treatment, (NH$_4$)$_3$AlF$_6$ starts to decompose and AlF$_3$ forms through several steps at different temperatures[15,19-27], as listed in Table 1.

For example, Rimkevich et al[19-21] indicated that (NH$_4$)$_3$AlF$_6$ formed by fluorination of kyanite or non-bauxite directly decomposed into AlF$_3$ at 275~282 or 320 ° C, respectively. However, Thorat[15], Makarov[18], Resentera[22], Kraidenko[23] and Shinn et al[24] indicated that a two-step progress occurs

**Table 1　Decomposition process of $(NH_4)_3AlF_6$**

| Mechanism | Reference | Reaction progress |
|---|---|---|
| One-step | [20, 21] | $(NH_4)_3AlF_6 \xrightarrow{275\sim282\,°C} AlF_3$ |
| | [19] | $(NH_4)_3AlF_6 \xrightarrow{320\,°C} AlF_3$ |
| Two-step | [22] | $(NH_4)_3AlF_6 \xrightarrow{194\,°C} NH_4AlF_4 \xrightarrow{220\,°C} AlF_3$ |
| | [15] | $(NH_4)_3AlF_6 \xrightarrow{227\,°C} NH_4AlF_4 \xrightarrow{286\,°C} AlF_3$ |
| | [18] | $(NH_4)_3AlF_6 \xrightarrow{275\,°C} NH_4AlF_4 \xrightarrow{345\,°C} AlF_3$ |
| | [23] | $(NH_4)_3AlF_6 \xrightarrow{250\,°C} NH_4AlF_4 \xrightarrow{355\,°C} AlF_3$ |
| | [24] | $(NH_4)_3AlF_6 \xrightarrow{170\,°C} NH_4AlF_4 \xrightarrow{300\,°C} AlF_3$ |
| Three-step | [25] | $(NH_4)_3AlF_6 \xrightarrow{194.9\,°C} NH_4AlF_4 \xrightarrow{222.5\,°C} (NH_4F)_{0.69}AlF_3 \xrightarrow{258.4\,°C} AlF_3$ |
| Several step | [26] | $(NH_4)_3AlF_6 \xrightarrow{175\,°C} NH_4AlF_4 \rightarrow AlF_3 \cdot (0.8\sim0.9)NH_4F \rightarrow AlF_3 \cdot (0.1\sim0.2)NH_4F \rightarrow AlF_3 \cdot (0.02\sim0.06)NH_4F \xrightarrow{310\,°C} AlF_3$ |

with the increment of temperature: $(NH_4)_3AlF_6 \rightarrow NH_4AlF_4 \rightarrow AlF_3$. Shinn et al[24] further pointed out that an intermediate phase with variable composition $AlF_3 \cdot (0.75\sim0.90)NH_4F$ may exist between $NH_4AlF_4$ and $AlF_3$. Hu et al[25] found that a three-step progress occurs: $(NH_4)_3AlF_6 \rightarrow NH_4AlF_4 \rightarrow (NH_4F)_{0.69}AlF_3 \rightarrow AlF_3$. However, Menz et al[26] found that the decomposition of $NH_4AlF_4$ is a multi-stage process and the range of existence of intermediates is expanded with the increment of pressure: $NH_4AlF_4 \rightarrow AlF_3 \cdot (0.8\sim0.9)NH_4F \rightarrow AlF_3 \cdot (0.1\sim0.2)NH_4F \rightarrow AlF_3 \cdot (0.02\sim0.06)NH_4F$. Resentera[22], Hu[25] and Menz[26] et al, further found that the increment of heating rate increases the corresponding decomposition tempe-rature. Therefore, the reaction process is quite complicated. Thus, the analysis of the fluorination process of $Al_2O_3$ by $NH_4HF_2$ and the decomposition of $(NH_4)_3AlF_6$ is beneficial to achieving an effective fluorination process.

In this work, the possible reactions involved during fluorination progress with different mass ratios of $NH_4HF_2$ to $Al_2O_3$ were simultaneously analyzed by thermogravimetry (TG), derivative thermogravimetry (DTG) and differential thermal analysis (DTA). The critical reaction temperatures of DTA curves under different mass ratios of $NH_4HF_2:Al_2O_3$ were determined. In addition, the morphologies and phases of the products obtained before and after the critical temperatures were prepared using direct thermal treatment and further analyzed.

## 1　Experiment

Commercially analytical grade $Al_2O_3$ (99.8wt%) and ammonium bifluoride (99.5wt% ) used in this study are from Sinopharm Group (China). According to reaction (1) and (2), the mass ratio of $NH_4HF_2:Al_2O_3$ for completed fluorination is 3.3530 and 2.2353, respectively. In order to investigate the reaction progress, two mass ratios were chosen for investigation: one is 2.5, which is higher than the value for the formation of $NH_4AlF_4$ but lower than that of $(NH_4)_3AlF_6$; the other is 3.5, which is higher than the value for the formation of $(NH_4)_3AlF_6$.

Thermalgravimetric analysis (TGA)-differential thermal analysis (DTA) of $Al_2O_3/NH_4HF_2$ mixtures were carried out in a Shimadzu DTG-60 unit at a rate of 5 °C/min from 25 °C to 600 °C under $N_2$ gas flow of 20 mL/min. DTG curves were obtained as the first derivative of the TGA curves.

After TGA-DTG-DTA analysis, the critical reaction temperatures of DTA curve were determined. In order to analyze the composition, morphologies and phases of products before and after each reaction stage, $Al_2O_3$ was firstly mixed with $NH_4HF_2$ (mass ratio of $NH_4HF_2: Al_2O_3$ is 2.5 or 3.5), put into a pure nickel crucible, and then placed in a modified tubular furnace consisting of a reactor and a two-zone condenser made from nickel (NP-2 grade) for fluorination test. The heating procedure was carried out at a rate of 5 °C/min under the flow of $N_2$ (purity>99%). Once the selected temperature was reached, the sample remained isothermally for 1 h, and then was cooled down to room temperature for further characterization.

The morphologies, composition and phases of $Al_2O_3$ powder, $NH_4HF_2$ agent and products obtained were analyzed by Camscan MX2600FE type-scanning electron microscopy with energy dispersive X-ray spectroscopy (SEM/EDS) (Oxford Instruments, INCA) and D/Max-2500 pc type X-ray diffraction (XRD).

## 2　Results and Discussion

### 2.1　Microstructure of as-received coating

Fig. 1a and Fig. 1b show the SEM morphology and the corresponding EDS results of $Al_2O_3$ powders. Clearly, $Al_2O_3$ particles exhibit nearly spherical morphology with average particle size of 80~100 μm, which is consistent with particle size analysis, as shown in Fig. 1c. EDS results in Fig. 1b further indicate that only Al and O are detected. The atom ratio of Al: O is close to 2:3, which coincides with the chemical formula of $Al_2O_3$. XRD patterns in Fig.2 verify that it is $Al_2O_3$, a mixture of highly disordered $α$-$Al_2O_3$ and $β$-$Al_2O_3$. However, the broad peak shows that some $Al_2O_3$ particles are of micro- or nano-size dimension. Fig. 3 shows the XRD pattern of $NH_4HF_2$ agent. The peaks are thin with a large ratio of peak to background, indicating that the structure is crystalline.

### 2.2　Thermal analysis of fluorination of $Al_2O_3$ with $NH_4HF_2$

Fig. 4 shows the TGA-DTG-DTA curves of $Al_2O_3/NH_4HF_2$ mixture with different mass ratios between 25 and 600 °C. Clearly, according to DTA curve, there are four apparent
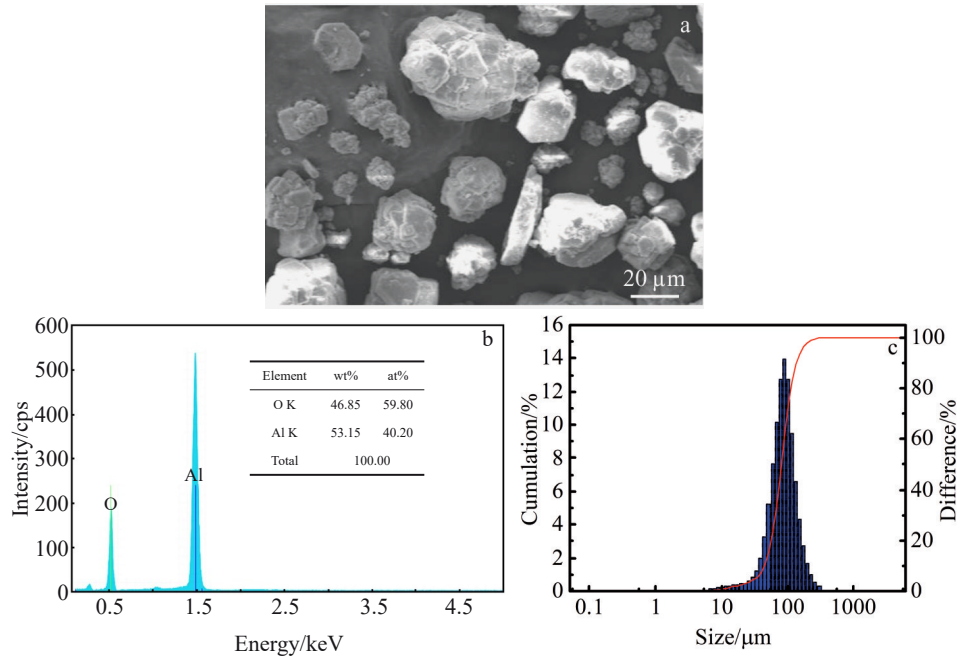
Fig.1 SEM image (a), corresponding EDS results of $Al_2O_3$ powder (b) and particle size analysis (c)
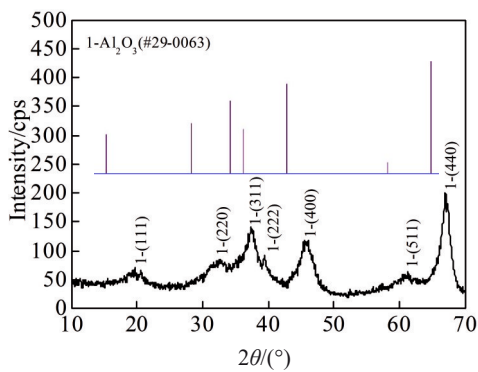


Fig.2 XRD patterns of $Al_2O_3$ powder
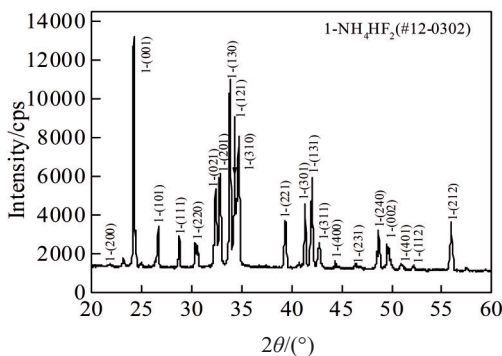


Fig.3 XRD patterns of $NH_4HF_2$ powder



Fig.4 TGA-DTG-DTA analysis of $Al_2O_3/NH_4HF_2$ mixtures with different mass ratios at 30~600 °C at a heating rate of 5 °C/min: (a) $NH_4HF_2$:$Al_2O_3$=2.5:1 and (b) $NH_4HF_2$:$Al_2O_3$=3.5:1

endothermic peaks between 25 and 600 °C and the mass ratio has no influence on the processes and the peak temperature: 126.8, 162.3~162.8, 249.8~250.1 and 356.8~357.7 °C. The first peak with minor mass loss at 126.8 °C is due to the melting of $NH_4HF_2$[22], which is partially overlapped with the second peak 2. Peaks 2~4 concede well with the peaks in the DTG curve with a large mass loss, especially for peaks 2~3. In this temperature range, $Al_2O_3$ does not decompose or change

structurally[27]. Above results indicate that the formation of peaks 2~4 is due to the chemical reaction. From TGA and DTG curves, it can be further found that the mass loss begins at the room temperature with appreciable rate and sharply increases at 126.8 °C, and then reaches the highest value at peak 2, suggesting the chemical reaction between $Al_2O_3$ and $NH_4HF_2$ to form fluorides. The total mass loss after peak 2 for both mass ratio of $NH_4HF_2$: $Al_2O_3$ is 22%~23%. After peak 2, the mass loss slowly increases to 230 °C, and increases sharply at peak 3 and ends at 273 °C, suggesting that a new reaction occurs. The mass loss during the peak 3 is 20.2% and 25.8% for the mass ratio of 2.5 and 3.5, respectively. After 273 °C, the mass loss slowly increases up to peak 4. For peak 4 at about 356.8 °C, another mass loss peak occurs again, indicating another chemical reaction. The mass loss during peak 4 for both mass ratio of $NH_4HF_2$: $Al_2O_3$ is 13.4%~14.4%. After 360 °C, only minor mass loss occurs and the residues at 600 °C are 43.4% and 37.6% for mass ratio of 2.5 and 3.5, respectively.

Based on above results, it can be found that three chemical reactions occur between 25 and 600 °C. The first chemical reaction starts at the room temperature, and sharply increases with the melting of $NH_4HF_2$, which dominates at 162.3~162.8 °C and is completed at 180 °C. The second chemical reaction starts at 235 °C, dominates at 249.8~250.1 °C and finishes at 273 °C. The third chemical reaction starts at 320 °C, dominates at 356.8~357.7 °C and is completed at 360 °C.
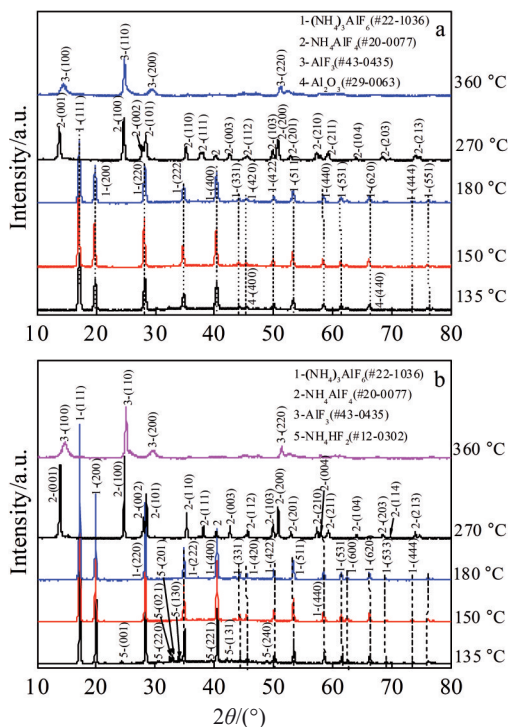
## 2.3 Characterization of the fluorination products of $Al_2O_3$

In order to identify and analyze the products involved in TGA-DTG-DTA curves of Fig. 4, samples produced using a modified tubular furnace at different temperatures before and after each peak in the DTA curves were analyzed by XRD, as shown in Fig. 5. Clearly, after 1 h heat treatment at 135 °C, $(NH_4)_3AlF_6$ (#22-1036) with minor $Al_2O_3$ is observed for low mass ratio of 2.5:1; while $(NH_4)_3AlF_6$ (#22-1036) with minor $NH_4HF_2$ (#12-0302) is observed for high mass ratio of 3.5:1. Between 150~180 °C, the peaks of $Al_2O_3$ and $NH_4HF_2$ at 135 °C significantly decrease and no new phases emerge under both mass ratios. At 270 °C, the peak of $Al_2O_3$ disappears and only $NH_4AlF_4$ is detected under both mass ratios. At 360 °C, the peak of $NH_4AlF_4$ disappears and only $AlF_3$ (#43-0435) is identified.

Above results indicate that the mass ratio of $NH_4HF_2$: $Al_2O_3$ has no influence on the critical chemical reaction temperature and phases of products. In this case, only the products at the mass ratio of 3.5 after heat treatment at different temperatures for 1 h were chosen for SEM/EDS analysis. Fig.6a is the SEM image of $Al_2O_3$/$NH_4HF_2$ mixtures after thermal treatment at 135 °C for 1 h. Clearly, faceted-grain particles with a size of 0.5~3 μm are observed. The average size is ~2.5 μm. With the increment of heat treatment temperature, the size of faceted-grain particles at 150 °C decreases to a mean size of 2 μm, as shown in Fig.6c. However, some particles larger than 2.5 μm form again after heat treatment at 180 °C for 1 h. EDS results in Fig.6b, Fig.6d and Fig.6f further indicate that the fluorides consist of Al, F and N without H due to detection limit. However, the content of Al increases with the increment of heat treatment temperature, suggesting the decomposition of $NH_4HF_2$ or the loss of $NH_4F$ from fluoride between 135~180 °C, which needs further investigation.

Fig. 7a and Fig. 7b show the SEM morphology and the corresponding EDS results of $Al_2O_3$/$NH_4HF_2$ mixtures after thermal treatment at 270 °C for 1 h, which is between peak 3 and peak 4 of DTA curve in Fig. 4. Clearly, finer spherical particles with a mean size of 0.5 μm form. Fig. 7b further indicates the fluorides consisting of Al, F and N, the same as fluorides produced at 135~180 °C. However, a high Al and low N content is observed, suggesting the further loss of $NH_4F$ from fluoride. Fig. 7c shows the SEM morphology of $Al_2O_3$/$NH_4HF_2$ mixtures after thermal treatment at 360 °C for 1 h, which is after peak 4 of DTA curve in Fig.4. Clearly, the size of spherical particle is further decreased compared to fluorides produced at 270 °C. EDS results in Fig.7d show that only Al and F are detected and the atomic ratio of F:Al is close to 3, consistent with the formal ratios of $AlF_3$.

## 2.4 Structure transformation of $AlF_3$

Fig. 8 shows the XRD patterns of $(NH_4)_3AlF_6$ mixtures after thermal treatment at 400 and 650 °C for 1 h. Clearly, two types of $AlF_3$ form: $\beta$-$AlF_3$ (#43-0435) at 400 °C and $\alpha$-$AlF_3$ (#44-0231) at 650 °C, indicating a structure transformation between 400~650 °C. From Fig.8, it can be further found that $\alpha$-$AlF_3$ (#44-0231) formed at 650 °C exhibits the highest intensity of the (012) orientation, indicating the formation of



Fig.5 XRD patterns of $Al_2O_3$/$NH_4HF_2$ mixtures after thermal treatment at different temperatures for 1 h: (a) $NH_4HF_2$:$Al_2O_3$= 2.5:1 and (b) $NH_4HF_2$:$Al_2O_3$=3.5:1
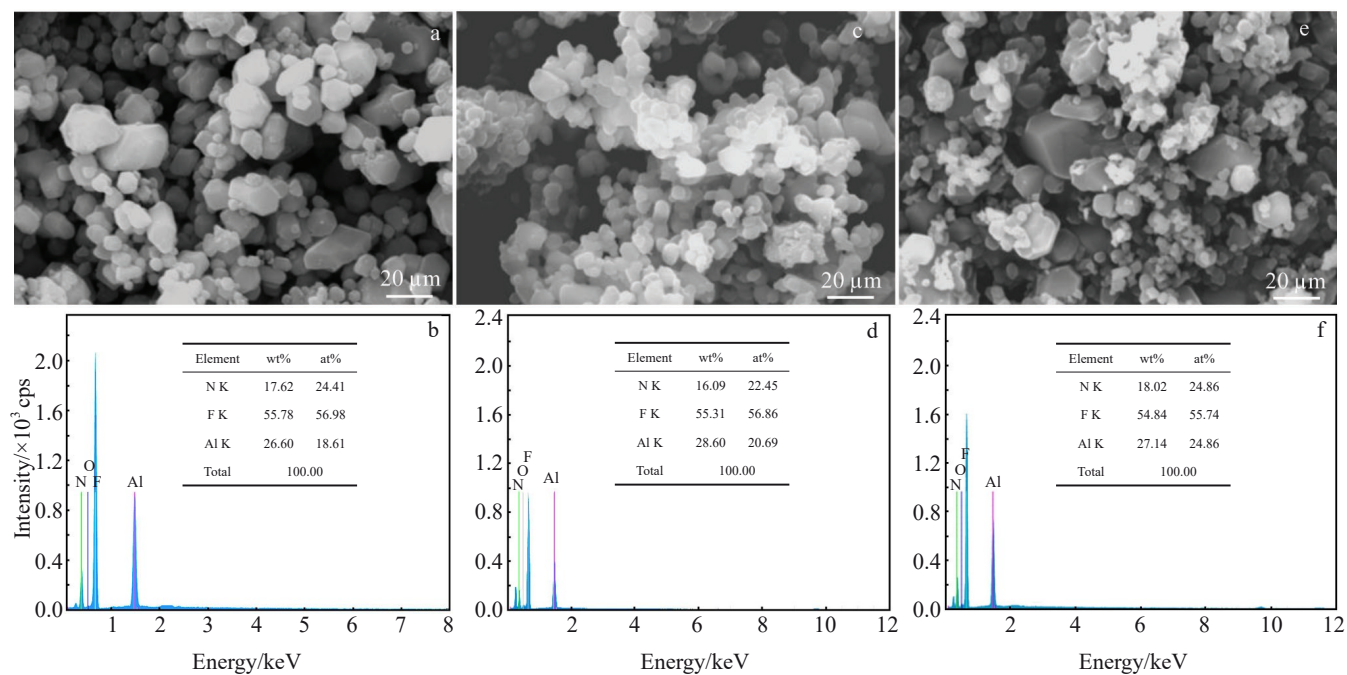
Fig.6　SEM morphologies (a, c, e) and corresponding EDS results (b, d, f) of $Al_2O_3$/$NH_4HF_2$ mixtures with mass ratio of $NH_4HF_2$:$Al_2O_3$=3.5 after thermal treatment at different temperatures for 1 h: (a, b) 135 °C, (c, d) 150 °C, and (e, f) 180 °C
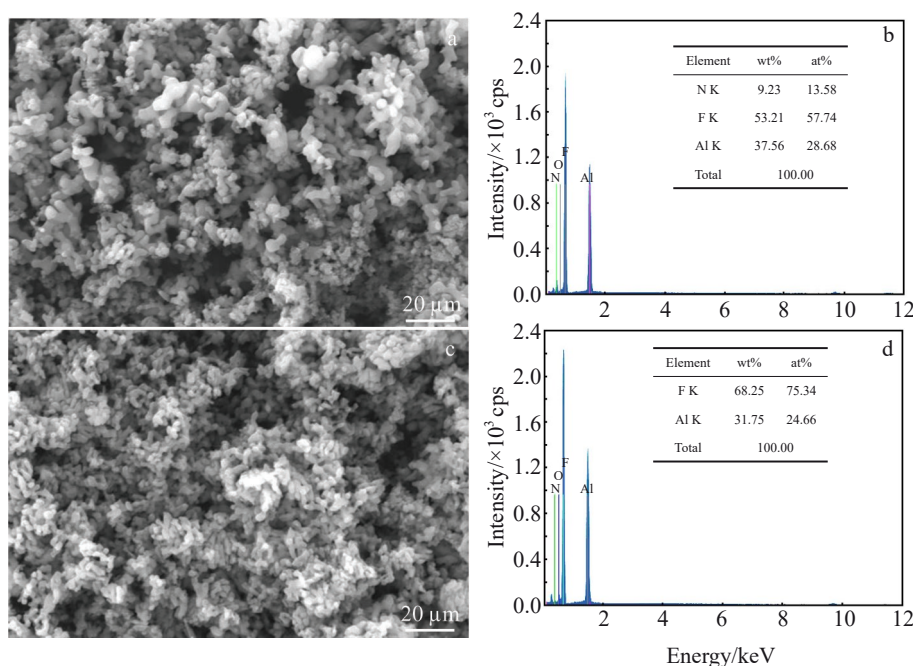


Fig.7　SEM morphologies (a, c) and corresponding EDS results (b, d) of $Al_2O_3$/$NH_4HF_2$ mixtures with mass ratio of $NH_4HF_2$:$Al_2O_3$=3.5 after thermal treatment at different temperatures for 1 h: (a, b) 270 °C and (c, d) 360 °C

$\alpha$-$AlF_3$ (#44-0231) along (012) preferred orientation.

Fig. 9 shows the SEM morphology and the corresponding EDS results of $AlF_3$ produced at 400 and 650 °C. Clearly, $AlF_3$ particles formed at 400 °C are still spherical, the same as that at 360 °C, but with a coarsesize, as seen in Fig.8a. The results indicate the coarsening of $\beta$-$AlF_3$ (#43-0435) particles. However, after the structure transformation, large rod-like $\alpha$- $AlF_3$

particles form at 650 °C because of the growth of $\alpha$-$AlF_3$ along (012) preferred orientation, as seen in Fig.9c. Fig.9b and Fig.9d indicate that both types of $AlF_3$ exhibit a comparable Al and F content with F:Al atomic ratio of 3.

**2.5　Discussion**

Results in Fig. 4 indicate that the first chemical reaction dominates at 162.2~162.8 °C (peak 2) and completes at 180 °C.
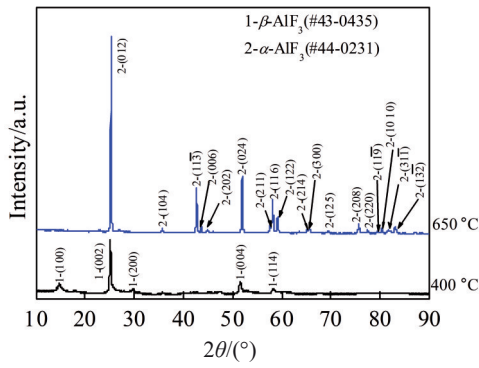
Fig.8    XRD patterns of $(NH_4)_3AlF_6$ after thermal treatment at 400 and 650 °C for 1 h

Fig.5 further indicate that the phases of products between 135~ 180 °C are $(NH_4)_3AlF_6$ with similar faceted-grain morphologies (Fig. 6). The mass ratio of $NH_4HF_2$ : $Al_2O_3$ has no influence on the chemical reaction progress and the products. Consequently, the formation of peak at 162.3~162.8 °C is due to the fluorination of $Al_2O_3$ to form $(NH_4)_3AlF_6$ according to chemical reaction (1)[15,19-22]. From Fig.4, it can be also found that the chemical reaction between $NH_4HF_2$ and $Al_2O_3$ solid powder begins at the room temperature. To confirm this assumption, an $NH_4HF_2/Al_2O_3$ mixture with mass ratio of 3.5 was prepared and analyzed by XRD right now or after one week at room temperature, as shown in Fig.10.

Clearly, no $(NH_4)_3AlF_6$ is detected after being mixed immediately; while $(NH_4)_3AlF_6$ besides $NH_4HF_2$ and $Al_2O_3$ form after being mixed for one week, the same as that at 135~ 180 °C (Fig.5). With the melting of $NH_4HF_2$ at 126.8 °C [22],

the reaction rate increases sharply due to higher liquid-solid reaction rate compared to lower solid-solid reaction rate. According to reaction (1), the mass ratio of $NH_4HF_2$ : $Al_2O_3$ for completed fluorination is 3.3530. Therefore, the fluorination is uncompleted for mass ratio of 2.5. That is why $Al_2O_3$ is detected in XRD pattern at 135 °C (Fig.5a). However, minor $NH_4HF_2$ is detected after 135 °C (Fig.5b), for mass ratio of 3.5 higher than 3.3530. With the increment of temperature, the decomposition and sublimation of $NH_4HF_2$ occur, so the XRD peak of $NH_4HF_2$ disappears at high temperature, as shown in Fig.5b.

Fig. 4 indicates that the second chemical reaction starts at 235 °C, dominates at 249.8~250.1 °C and is completed at 273 °C, which coincides well with the value in Ref.[23] and is close to the value in Ref. [18]. Results in Fig. 5 and Fig. 7 further indicate that only $NH_4AlF_4$ (#20-0077) with finer grain size of 0.5 µm is observed at 270 °C, suggesting the decomposition of $(NH_4)_3AlF_6$ to form $NH_4AlF_4$ at 249.8 °C through the following reaction:

$$(NH_4)_3AlF_6 = NH_4AlF_4 + 2NH_4F \uparrow \tag{3}$$
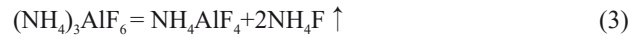
For low mass ratio of 2.5, part of $Al_2O_3$ powder is not fluoridated. Thus, the residue consists of $NH_4AlF_4$ and original $Al_2O_3$ at 270 °C. The theoretical calculation indicates that the mass of residue is 57.8%, which coincides with the measured value of 56.8%, as shown in Fig.4a. However, for high mass ratio of 3.5, all $Al_2O_3$ powder is fluoridated and the residue at 270 °C is $NH_4AlF_4$. In this case, the mass of $NH_4AlF_4$ residue at 270 °C is 52.7%, which is close to the measured value of 52.2%, as shown in Fig.4b.

Based on TG-DTA results in Fig.4, the residue at 270 °C for low mass ratio of 2.5 should contain minor un-reacted $Al_2O_3$. However, the decomposition $(NH_4)_3AlF_6$ will form $NH_4F$,
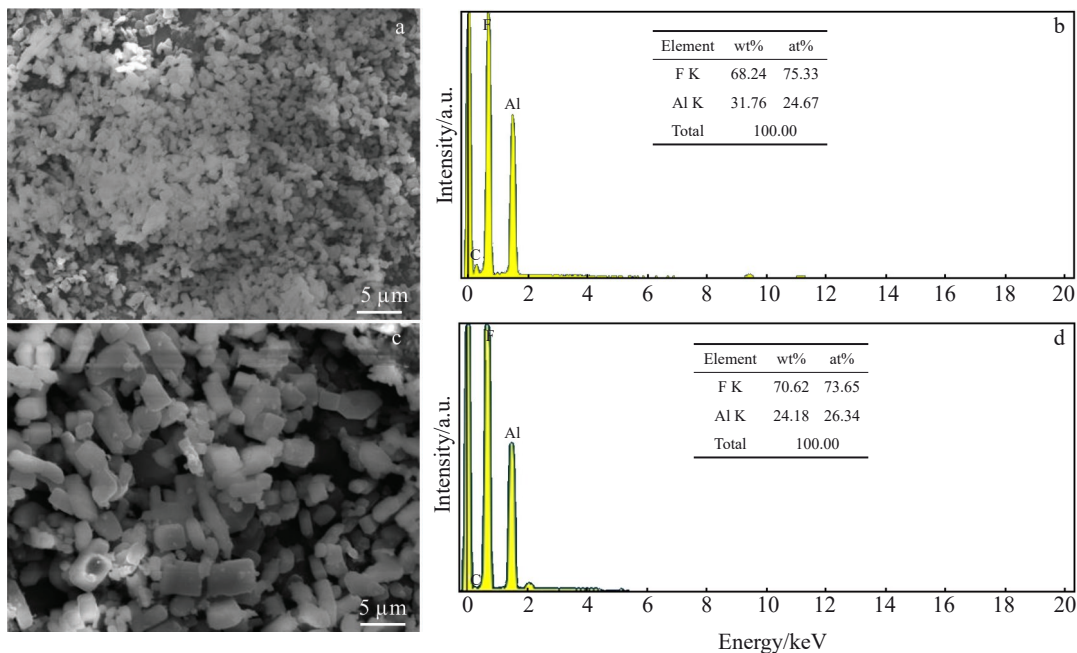


Fig.9    SEM morphologies (a, c) and corresponding EDS results (b, d) of $(NH_4)_3AlF_6$ after thermal treatment at different temperatures for 1 h: (a, b) 400 °C and (c, d) 650 °C
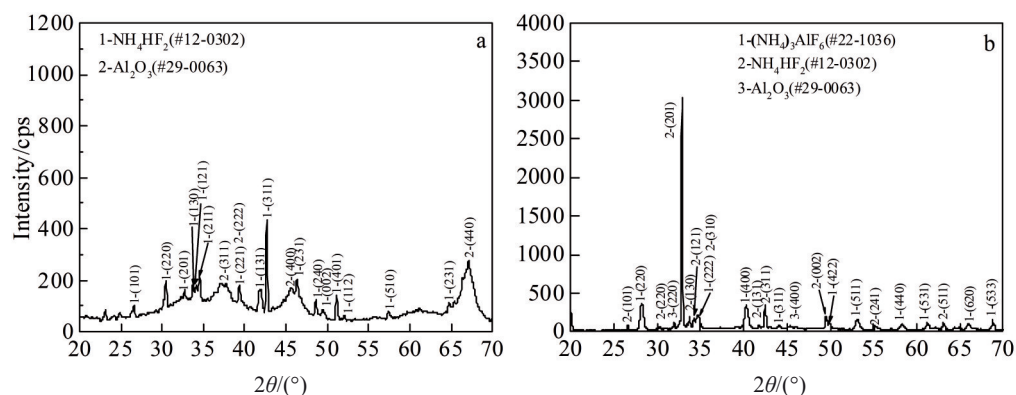
Fig.10　XRD patterns of $Al_2O_3/NH_4HF_2$ mixtures with the mass ratio of $NH_4HF_2$:$Al_2O_3$=3.5 at room temperature: (a) after mixing and (b) after mixing for one week

which can further react with un-reacted $Al_2O_3$ to form $NH_4AlF_4$ according to following reaction:

$$Al_2O_3+8NH_4F=2NH_4AlF_4+3H_2O\uparrow+6NH_3\uparrow \qquad (4)$$

That is why no $Al_2O_3$ is detected from the XRD pattern at 270 °C (Fig.5b).

With further increase in temperature, the third chemical reaction starts at 320 °C, dominates at 356.8~357.7 °C and is completed at 360 °C, which coincides well with the value in Ref. [18, 23]. Fig. 5 indicates that only $AlF_3$ (#43-0435) is identified at 360 °C. Fig.7 shows that the grain size is further refined compared to $NH_4AlF_4$ formed at 270 °C. Based on above results, it can be concluded that the formation of peak at 356.8~357.7 °C is due to the decomposition of $NH_4AlF_4$ to form $AlF_3$ through the following reaction:

$$NH_4AlF_4=AlF_3+NH_4F\uparrow \qquad (5)$$

Therefore, $AlF_3$ forms at 360 °C. TG-DTA results in Fig.4 exhibit that $AlF_3$ is stable without chemical change up to 600 °C; while the release of adsorbent such as F will cause minor mass loss. The fluorination is uncompleted for low mass ratio of 2.5, and then the residue at 600 °C is $AlF_3$ with minor un-reacted $Al_2O_3$. The theoretical calculation indicates that the residue for low mass ratio of 2.5 is 42.3%, which coincides well with the measured value of 43.4%, as shown in Fig. 4a. However, all $Al_2O_3$ powder is fluoridated for high mass ratio of 3.5, and the residue is $AlF_3$. In this case, the calculated residue at 600 °C is 36.6%, which is close to measured value of 37.6%, as shown in Fig. 4b. Even though no chemical reaction occurs for $AlF_3$ at 360~600 °C, a structure transformation from $\beta$-$AlF_3$ (#43-0435) to $\alpha$-$AlF_3$ (#44-0231) occurs at 456 °C[28], which causes the growth of rod-like $AlF_3$ (Fig. 9) along (012) preferred orientation, as seen in Fig.8.

## 3　Conclusions

1) The mass ratio of $NH_4HF_2$:$Al_2O_3$ has no influence on the critical reaction temperature and reaction process.

2) The fluorination starts at room temperature with the formation of $(NH_4)_3AlF_6$, dominates at 162.3~162.8 °C and is completed at 180 °C.

3) $(NH_4)_3AlF_6$ starts to decompose sequentially through a two-step decomposition reaction with the formation of $NH_4AlF_4$ at 249.8~250.1 °C and finally decomposes to $\beta$-$AlF_3$ at 356.8~357.7 °C.

4) The transformation from $\beta$-$AlF_3$ to $\alpha$-$AlF_3$ occurs between 400~650 °C.

## References

1　Tron A, Park Y D, Mun J Y. *Journal of Power Sources*[J], 2016, 325: 360

2　Luo Z Y, Lei W X, Wang X *et al. Journal of Alloys and Compounds*[J], 2020, 812: 152 132

3　Zhu X, Zhu G, Chen W *et al. Journal of the Optical Society of America B*[J], 2017, 34: 15

4　Yan H, Yang J, Li W *et al. Metallurgical and Materials Transactions*[J], 2011, 42: 1

5　Menz D H, Zacharias A, Kolditz L. *Journal of Thermal Analysis* [J], 1988, 33: 811

6　Menz D H. *Journal of Thermal Analysis*[J], 1992, 38: 321

7　Zhang J S, Qiu Z X. *Light Metals*[J], 1988, 6: 10

8　Karelin V A, Strashko A N, Dubrovin A V *et al. Procedia Chemistry*[J], 2014, 11: 56

9　Konarov A, Kim H J, Yashiro H *et al. Journal of Materials Chemistry A*[J], 2019, 7: 13 012

10　Dreveton A. *Procedia Engineering*[J], 2012, 46: 255

11　Krysztafkiewicz A, Rager B, Maik M. *Journal of Hazardous Materials*[J], 1996, 48: 31

12　Qu Xinxin, Ma Liqun, Jin Chuanwei *et al. Rare Metal Materials and Engineering*[J], 2011, 40(3): 543 (in Chinese)

13　Scholz G, Kemnitz E. *Solid State Sciences*[J], 2009, 11: 676

14　Rimkevich V S, Girenko I V, Pushkin A A. *Russian Journal of Applied Chemistry*[J], 2013, 86: 1470

15　Thotat D D, Tripathi B M, Sathiyamoorthy D. *Hydrometallurgy* [J], 2011, 109(1-2): 18

16　Mukherjee A, Awasthi A, Mishra S *et al. Thermochimica Acta* [J], 2011, 520: 145

17  Andreev A A, Diachenko A N. *Theoretical Foundations of Chemical Engineering*[J], 2009, 43: 707

18  Makarov D V, Belyaevskii A T, Menshikov Yu P *et al. Russian Journal of Applied Chemistry*[J], 2007, 80: 175

19  Rimkevich V S, Pushkin A A, Malovitskii Yu N *et al. Russian Journal of Applied Chemistry*[J], 2009, 82: 6

20  Rimkevich V S, Pushkin A A, Girenko I V *et al. Russian Journal of Non-Ferrous Metals*[J], 2014, 55: 344

21  Rimkevich V S, Girenko I V, Pushkin A A. *Russian Journal of Applied Chemistry*[J], 2013, 86: 1470

22  Resentera A C, Rosales G D, Esquivel M R *et al. Thermochimica Acta*[J], 2020, 689: 178 609

23  Kraidenko R I. *Fluorine-Ammonium Division of Multi-Component Silicate Systems to Individual Oxides*[D]. Russia: Tomsk Politechnical University, 2008

24  Shinn D B, Crocket D S, Haendler H M. *Inorganic Chemistry*[J], 1966, 5: 1927

25  Hu X W, Li L, Gao B L *et al. Transactions of Nonferrous Metals Society of China*[J], 2011, 21: 2087

26  Menz D H, Bentrup U. *Zeitschrift für Anorganische und Allgemeine Chemie*[J], 1989, 576: 186

27  Abdullah A A, Oskierski H C, Altarawneh M *et al. Minerals Engineering*[J], 2019, 140: 105 883

28  König R, Scholz G, Scheurell K *et al. Journal of Fluorine Chemistry*[J], 2010, 131: 91

## NH₄HF₂氟化Al₂O₃制备无水AlF₃研究

李成硕，孟君晟，陈明宣，史晓萍，李　晓，马　强

(山东交通学院 船舶与港口工程学院，山东 威海 264200)

**摘　要：** 采用热重-差热分析（TG-DTA）方法对不同 $NH_4HF_2/Al_2O_3$ 质量比的 $Al_2O_3+NH_4HF_2$ 混合物的热行为进行了分析，确定了DTA曲线的临界温度。进一步分析了各临界温度前后直接热处理所得产物的形貌和物相。结果表明，质量比对临界反应温度和反应过程没有影响。氟化反应在室温下以 $(NH_4)_3AlF_6$ 的形成开始，在162.3~162.8 ℃时占主导地位，在180 ℃左右完成。进一步热处理后，$(NH_4)_3AlF_6$ 在249.8~250.1 ℃分解为 $NH_4AlF_4$，在356.8~357.7 ℃分解为 $\beta\text{-}AlF_3$；随后 $\beta\text{-}AlF_3$ 在400~650 ℃向 $\alpha\text{-}AlF_3$ 转变。

**关键词：** 氟化氢铵；氟化；热分解；氟化铝